

Two-scale modeling of granular materials: a DEM-FEM approach

Michał Nitka · Gaël Combe · Cristian Dascalu ·
Jacques Desrues

Received: 8 October 2010
© Springer-Verlag 2011

Abstract The presented study considers a two-scale numerical scheme for the description of the behavior of granular materials. At the small-scale level, the granular structure consists of 2D round rigid grains, modeled by the Discrete Element Method (DEM). At the macroscopic level, we consider a numerical solution obtained with the Finite Element Method (FEM). The link between scales is made using a computational homogenization method, in which the average REV stress response of the granular micro structure, together with the tangent moduli, are obtained in each macroscopic Gauss point of the FEM mesh as the result of the macroscopic deformation history imposed to the REV. In this way, the numerical constitutive law and the corresponding tangent matrix are obtained directly from the discrete behavior of the microstructure. We discuss the principle of the computational homogenization applied to this association of FEM with DEM and we present examples of the two-scale computations, like drained and undrained biaxial tests.

Keywords Granular materials · Computational homogenization · Discrete elements · Finite elements

M. Nitka · G. Combe · C. Dascalu · J. Desrues (✉)
3SR Lab, UJF-Grenoble 1, Grenoble-INP, CNRS UMR 5521,
38041 Grenoble, France
e-mail: jacques.desrues@grenoble.cnrs.fr

M. Nitka
e-mail: micnitka@pg.gda.pl

G. Combe
e-mail: gael.combe@hmg.inpg.fr

C. Dascalu
e-mail: cristian.dascalu@hmg.inpg.fr

1 Introduction

The continuum modeling of the macroscopic response of granular materials, as a consequence of the interactions of individual grains at the micro scale, is the object of this paper. A two scale numerical homogenization approach is considered. At the small-scale level, a granular structure is defined as a Representative Element Volume (REV), while at the large-scale level a continuum description is adopted. This granular system can be simulated using a Discrete Element Method (DEM). For a given history of the deformation gradient, the method allows computation of the global stress response of the REV. At the macroscopic level, a numerical solution for the boundary value problem is obtained using the Finite Element Method (FEM). The upscaling technique consists of using the DEM model at each Gauss point of the FEM mesh to derive numerically the constitutive response. In this process, a tangent operator is generated together with the stress increment corresponding to the given strain increment.

In recent years, many authors proposed two-scale approaches for granular materials. The formalism proposed in the present contribution is close to the one in Borja and Wren [1] and Wren and Borja [2]. These important contributions consider the analysis of the homogenized response of granular microstructures in a macroscopic point. The present work continues this modeling strategy by considering two-scale computation with FEM solutions for the macroscopic problems. We also mention the works of Miehe et al. [3], which considers dynamic relaxation stabilization techniques and Meier et al. [4] which explicitly calculate the tangent operator. The present formulation is also connected to our previous results [5], where a continuum description was assumed for the granular microstructure.

56 Elementary tests (oedometric, shear and biaxial) were per-
 57 formed to evaluate the capabilities of this method. A selection
 58 of results of these tests is presented in the paper.

59 2 Macroscopic formulation

60 2.1 Macroscopic constitutive law

61 A quasistatic finite strain continuum formulation is consid-
 62 ered at the macroscopic level. The constitutive response at
 63 this level is obtained from DEM computations in the REV.

64 For a given history of macroscopic deformation gradient
 65 $\bar{\mathbf{F}}$, the macroscopic Cauchy stress $\bar{\sigma}$ results from microscopic
 66 forces between grains through an average formula, as shown
 67 in the next section. Written in terms of the Piola–Kirchhoff
 68 stress $\bar{\mathbf{P}} = J\bar{\sigma}\bar{\mathbf{F}}^{-T}$, with $J = \det(\bar{\mathbf{F}})$, the effective constitu-
 69 tive behavior expresses the stress as a function of the history
 70 of the deformation gradient:

$$71 \bar{\mathbf{P}}(t) = \Gamma^t\{\bar{\mathbf{F}}(\tau), \tau \in [0, t]\} \quad (1)$$

72 We assume that, for any given history of $\bar{\mathbf{F}}$ till time t , $\bar{\mathbf{P}}(t)$
 73 admits a right time derivative $\dot{\bar{\mathbf{P}}}$:

$$74 \dot{\bar{\mathbf{P}}} = \lim_{\delta t \rightarrow 0} \frac{\bar{\mathbf{P}}(t + \delta t) - \bar{\mathbf{P}}(t)}{\delta t} \quad (2)$$

75 and that the right-sided derivative $\dot{\bar{\mathbf{P}}}$ depends only on the right
 76 time derivative $\dot{\bar{\mathbf{F}}}$, that is:

$$77 \dot{\bar{\mathbf{P}}} = \Theta(\dot{\bar{\mathbf{F}}}) \quad (3)$$

78 The function Θ is generally non-linear with respect to its
 79 argument $\dot{\bar{\mathbf{F}}}$.

80 For a given rate of deformation gradient $\dot{\bar{\mathbf{F}}^0}$, assuming
 81 that Θ is differentiable at $\dot{\bar{\mathbf{F}}^0}$, we can construct the material
 82 tangent moduli:

$$83 B_{ijkl} \left(\dot{\bar{\mathbf{F}}^0} \right) = \frac{\partial \Theta_{ij}}{\partial \dot{F}_{kl}} \Big|_{\dot{\bar{\mathbf{F}}} = \dot{\bar{\mathbf{F}}^0}} \quad (4)$$

84 where capital indices refer to Lagrangian variables and small
 85 indices refer to Eulerian variables, respectively.

86 2.2 Numerical integration

87 At the macroscopic scale, finite elements are employed to
 88 solve the homogenized problem. When an incremental lin-
 89 earization procedure is adopted for the obtained non-lin-
 90 ear problem, the constitutive function Θ and its derivatives
 91 should be evaluated numerically in each integration (Gauss)
 92 point. We describe here this numerical procedure.

93 During each time step, from t to $t + \Delta t$, in every Gauss
 94 point, the increment of deformation gradient $\Delta\bar{\mathbf{F}} = \dot{\bar{\mathbf{F}}}\Delta t$ is

transmitted to the microstructure. As the result of DEM computations, the Piola–Kirchhoff stress $\bar{\mathbf{P}}(t + \Delta t)$ is returned at each Gauss point and the corresponding stress rate is computed as

$$95 \Theta^d(\dot{\bar{\mathbf{F}}}) = \frac{\bar{\mathbf{P}}(t + \Delta t) - \bar{\mathbf{P}}(t)}{\Delta t} \quad (5) \quad 99$$

100 giving the discrete version of the constitutive function Θ in
 101 Eq. 3.

102 A second step in the integration procedure at the level of
 103 a macroscopic Gauss point concerns the computation of the
 104 material tangent moduli B_{ijkl} needed in a typical Newton–
 105 Raphson algorithm. Since the derivatives in the relation (4)
 106 involve the function Θ which is itself computed as a deriva-
 107 tive in Eq. 5, the tangent moduli should be computed in two
 108 steps.

109 For a given $\dot{\bar{\mathbf{F}}}$, we perform a first step in which we com-
 110 pute $\dot{\Theta}_{ij}^d(\dot{\bar{\mathbf{F}}})$, as described previously in the formula (5). This
 111 corresponds to the increment of deformation gradient $\dot{\bar{\mathbf{F}}} =$
 $\dot{\bar{\mathbf{F}}}\Delta t$.

112 Then, we consider perturbed increments of deformation
 113 gradient $\Delta\bar{F}_{kl}^* = \Delta\bar{F}_{kl} + \varepsilon\Delta t\Delta^{kl}$, where Δ^{kl} is a second-
 114 order (two-point) tensor such that all its components are equal
 115 to 0 except the kL one which is equal to 1. Here ε is a small
 116 parameter. This second step corresponds to a rate of defor-
 117 mation gradient $\dot{\bar{F}}_{kl}^* = \dot{\bar{F}}_{kl} + \varepsilon\Delta^{kl}$. Following again the
 118 formula (5), we compute $\dot{\Theta}_{ij}^d(\dot{\bar{F}}_{kl} + \varepsilon\Delta^{kl})$. In this second
 119 step, computations are performed for all different values of
 120 k and L , i.e. 4 computations in the two-dimensional case.

121 Finally, the results of these two steps allow for the com-
 122 putation of material tangent moduli

$$123 B_{ijkl}^d = \frac{\dot{\Theta}_{ij}^d(\dot{\bar{F}}_{kl} + \varepsilon\Delta^{kl}) - \dot{\Theta}_{ij}^d(\dot{\bar{F}})}{\varepsilon} \quad (6) \quad 124$$

125 as a discrete version of the formula (4).

126 This procedure is performed in every time step and in
 127 every Gauss point of the macroscopic finite element discret-
 128 ization. For a more detailed presentation of this numerical
 129 procedure, we refer the reader to Bilbie et al. [5].

130 3 Micro-scale formulation

131 The granular assembly is made of a set of N polydisperse
 132 discs, with the diameters uniformly distributed between a
 133 and $a/2$. Particle motion are time-discretized with 3rd order
 134 predictor-corrector scheme [9]. All grains interact via linear
 135 elastic laws and Coulomb friction when they are in contact
 136 [6]: the normal contact force f_n is related to the normal appar-
 137 ent interpenetration δ of the contact as $f_n = k_n\delta$, where k_n is
 138 a normal stiffness coefficient ($\delta > 0$ if a contact is present,
 139 $\delta = 0$ if there is no contact). The tangential component f_t
 140 of the contact force is proportional to the tangential elastic

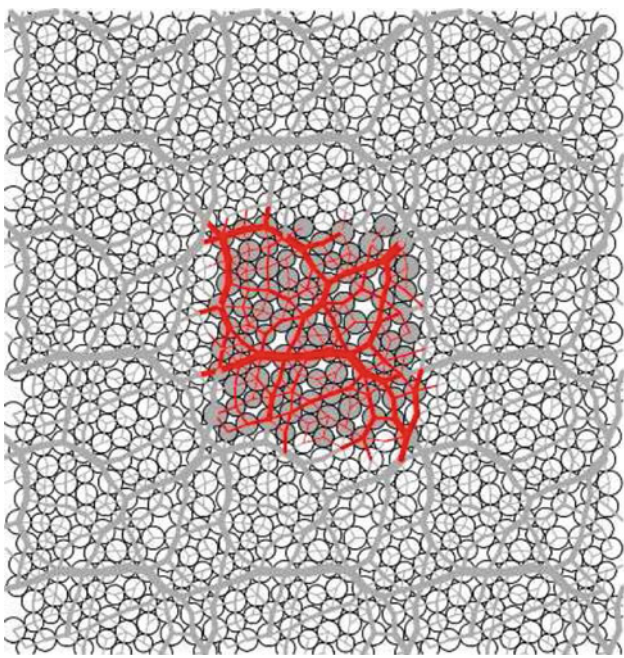


Fig. 1 Illustration of a sample (REV) of 100 discs (gray particles), with periodic boundary conditions (PBC), under isotropic loading. The normal contact forces are shown in red (lines thickness are proportional to force intensity). The PBC are illustrated by reproducing periodically the REV (white discs - light gray forces)

relative displacement, with a tangential stiffness coefficient k_t . The Coulomb condition $|f_t| \leq \mu f_n$ requires an incremental evaluation of f_t in each time step, which leads to some amount of slip each time one of the equalities $f_t = \pm \mu f_n$ is imposed [6]. In that study, k_n is such that $\kappa = k_n/\sigma_0 = 1,000$ [11], where σ_0 is the 2D isotropic pressure. The stiffness ratio is $k_t/k_n = 1$. The intergranular angle of friction is $\mu = 0.5$. A normal viscous component opposing the relative normal motion of any pair of grains in contact is also added to the elastic force f_n to obtain a critical damping of the dynamics when equilibrium states are computed. The *Periodic Boundary Conditions* (PBC) (Fig. 1) are used.

By imposing changes of the periodic box, strains are imposed to the granular media. Resulting macroscopic Cauchy stresses are evaluated using the classical average formula: $\sigma_{ij} = \frac{1}{S} \sum_{c=1}^{N_c} f_i^c \cdot l_j^c$, where S is the area of the sample, f_i^c and l_j^c are respectively the component i of the contact force f acting in c and the component j of the branch vector l joining the mass centers of two grains in contact [7].

4 Numerical results

The FEM-DEM method was implemented in the FEM code *FlagsHyp* [8]. The implementation involved significant modifications in the original code, but essentially it consisted in adding the DEM code as a constitutive module. A driver routine allows for generating from the DEM both the stress

response and the tangent stiffness operator, according to Sect. 2. For the tests presented, the 2D quadratic element with four Gauss points was chosen. A very simple mesh with 4 elements was used. On the micro level, in DEM calculations, the number of grains in the REV cell was 400, a very low number in order to reduce the CPU time.

Initially the REV is assigned a (isotropic) stress state at the microscopic scale by (isotropically) compressing under kinematical control up to a certain stress state. Accordingly, the stress state at the integration point in the FEM element should be equal to the microscopic stress. For a homogeneous test, this must be true in all the elements of the mesh, but also the boundary stress applied must be equal on the stress-controlled boundaries. The macroscopic stress in every Gauss point is equal to the microscopic response $\Sigma_{ij} = \sigma_{ij}$, where Σ_{ij} is a macroscopic stress and σ_{ij} is a microscopic stress. On the macroscopic boundary the isotropic compression is applied to balance microscopic stresses.

Different tests were performed using the multi-scale scheme, modeling typical laboratory tests like oedometer, biaxial tests, shear test. All macroscopic results were compared to the direct DEM computations on one periodic assemblage of 2D disks. We present first the oedometer and then the biaxial test simulations, in two very different cases which are respectively the “drained” and the “undrained” case. In soil mechanics, soils are often saturated by water and their response is quite different depending whether the water is free to flow through the soil (drained case, free volumetric strain for the skeleton), or trapped within it (undrained case, i.e. zero volume change).

The first case is an oedometric test. The lateral faces are fixed but frictionless, the top face is displaced downward. Results are plotted in Fig. 2. The vertical stress increases indefinitely, which is expected since (i) this path is not leading to plastic flow and (ii) no mechanism for degradation of the grains (e.g. grain fracture, attrition,...) has been introduced in the microscopic behaviour. $K_0 = \sigma_{xx}/\sigma_{yy}$ is plotted as a function of vertical strain. For the isotropic case it is related to the Poisson ratio through $K_0 = v/(1-v)$. The value (0.4–0.5) is known to correspond to uncemented solids [12]. DEM results and multi scale computations FEM-DEM are very close to each other.

The second case is a biaxial test under so-called “drained condition”. A constant pressure $\sigma_{lat} = \sigma_0$ is applied on the lateral faces, while the top face is displaced downward. Using the symmetry of the problem, only the upper left quarter of the specimen is computed. The bottom face is perfectly lubricated (no friction) in a first test—FEM-DEM (lubr_ends), but in a second test FEM-DEM (frict_ends) the friction was allowed to develop. The lubricated case on Fig. 3 shows a typical biaxial test response, with a peak stress around 0.014, and a volumetric strain curve exhibiting contractancy first, then strong dilatancy after a minimum around 0.0025. One can

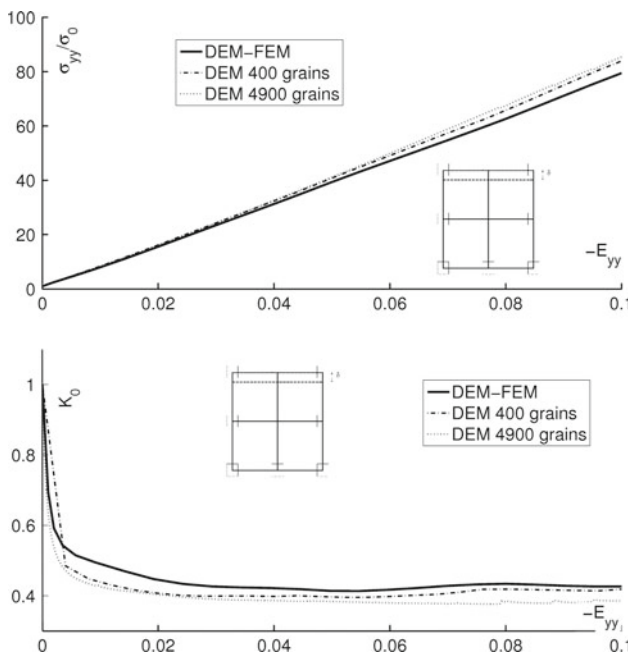


Fig. 2 Multi scale computations for oedometric test. Subplots indicate the displacement boundary conditions: blocked, sliding, prescribed (dashed lines)

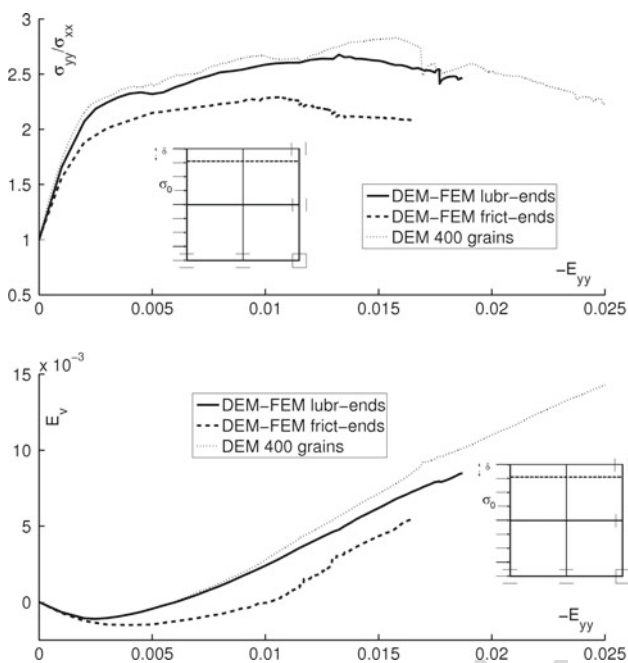


Fig. 3 Multi scale computations for classical biaxial test. Subplots indicate the boundary conditions, arrows means pressure controlled

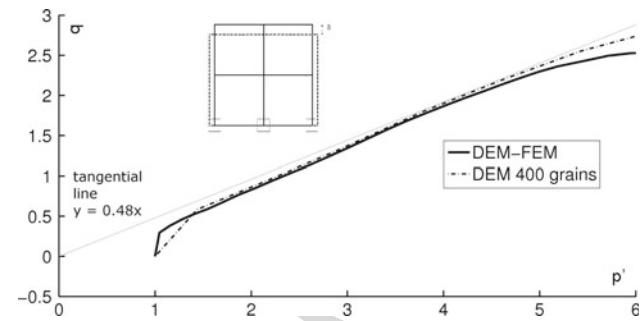


Fig. 4 Multi scale computations for biaxial test without volume changes

macroscopic scale, and differs essentially from the elementary response given by the DEM.

Next, a so-called undrained biaxial test was performed, i.e. a biaxial without volume changes. The top wall was compressing the sample, when the left and right one were extending. This kind of test is usually presented in the (q, p') plane, with q the deviatoric stress and p' the mean effective stress. The results presented in Fig. 4 shows a typical dense sand undrained response, with a stress path reaching shortly a straight line, and then going up along this line, due to the constrained dilatancy that induces a strong increase of the mean effective stress.

5 Conclusions

A two-scale numerical approach for granular materials has been presented, combining DEM modeling of the granular microstructure with the FEM modeling at the macroscopic level. We showed that FEM-DEM computations, with numerically calculated tangent matrix, are reliable at least for simple cases. In a series of tests, the response after peak has been obtained. The results are consistent with those obtained directly from DEM computations. A large number of tests, not reported here, with different numerical parameters, steps size, convergence indicators, have shown robustness of the overall numerical responses. Convergence can become difficult in some configurations. However, further improvements in the numerical strategy, and extensive exploration of the sensitivity of the method to some numerical parameters, like those controlling the perturbations in the numerical derivation of the tangent matrix, may change the balance in terms of efficiency between DEM computations and the presented FEM-DEM method for more complex geotechnical problems.

References

1. Borja, R.I., Wren, J.R.: Macromechanics of granular media Part I: Generation of overall constitutive equation for assemblies of circular disks. *Comput. Methods Appl. Mech. Eng.* **127**, 13–36 (1995)

- 260 2. Wren, J.R., Borja, R.I.: Macromechanics of granular media Part 277
261 II: Overall tangential moduli and localization model for peri- 278
262 odic assemblies of circular disks. *Comput. Methods Appl. Mech. 279*
263 Eng.
- 264 141, 221–246 (1997)
- 265 3. Miehe, C., Dettmar, J., Zah, D.: Homogenization and two-scale 280
266 simulations of granular materials for different microstructural 281
267 constraints. *Int. J. Num. Meth. Eng.* 83, 1206–1236 (2010)
- 268 4. Meier, H.A., Steinmann, P., Kuhl, E.: Towards multiscale 282
269 computation of confined granular media—contact forces, stresses and 283
270 tangent operators. *Techn. Mech.* 28, 32–42 (2008)
- 271 5. Bilbie, G., Dascalu, C., Champon, R., Caillerie, D.: Micro-fracture 284
272 instabilities in granular solids. *Acta Geotech.* 3, 25–35 (2008)
- 273 6. Cundall, P.A., Strack, O.D.L.: A discrete numerical model for 285
274 granular assemblies. *Géotechnique* 29(1), 47–65 (1979)
- 275 7. Christoffersen, J., Mehrabadi, M.M., Nemat-Nasser, S.: A 286
276 micromechanical description of granular material behavior. *J. Appl. Mech., Trans. ASME* 48(2), 339–344 (1981)
- 277 8. Bonnet, J., Wood, R.D.: Nonlinear Continuum Mechanics for 278
278 Finite Element Analysis. pp. 53–117. Cambridge University Press, 279
Cambridge (1997)
- 279 9. Allen, M.P., Tildesley, D.J.: Computer Simulation of Liquids. 280
Oxford Science, Oxford (1994)
- 280 10. Ellero, M.: Smoothed Particle Dynamics Methods for the Simula- 281
282 tion of Viscoelastic Fluids, pp. 3–10. Thesis of Berlin University, 283
(2004)
- 283 11. Combe, G., Roux, J.-N.: Discrete numerical simulation, quasi- 284
284 static deformation and the origins of strain in granular materials. In: DiBenedetto, H., Doanh, T., Geoffroy, H., Sauzeat, C. (eds.), 285
3rd International Symposium on Deformation Characteristics of 286
Geomaterials, pp. 1071–1078. Lyon, France, (2003)
- 287 12. Castellanza, R., Nova, R., Arroyo, M.: Oedometric testing and com- 288
288 paction bands in cemented soils. *J. Japanese Geotech. Soc. Soils 289*
Found. 45(2), 181–194 (2005)
- 290 291
- 292